Nanostructure Self-Assembly as an Emerging Technology

James L. Merz
Dept. of Electrical Engineering, Univ. of Notre Dame, Notre Dame, IN 46556

Albert-László Barabási, Jacek K. Furdyna
Dept. of Physics, Univ. of Notre Dame, Notre Dame, IN 46556

R. Stanley Williams
Quantum Structures Research Initiative, Hewlett-Packard Laboratories, Palo Alto, CA 94304

1. Introduction

In this article a brief review will be given of the growth and properties of self-assembled quantum dots (SAQDs). The current understanding of the growth mechanisms will be described, and some of the techniques that might be used to control the growth will be discussed. Emphasis will be placed on controlling the nucleation and growth of these self-assembled quantum dots as a means to produce ordered arrays. Finally, a brief discussion will be given of possible applications of arrays of SAQDs.

2. Comments on the growth of SAQDs

Several different semiconductor systems will be considered in this paper including InAs quantum dots on GaAs, CdSe dots on ZnSe, and Ge dots grown on Si. The relationship between band gap and lattice constant is well known for a large number of compounds and Group IV semiconductors. The relative mismatch between the InAs and GaAs lattices is approximately 6.9%, slightly less than 7% for CdSe/ZnSe, and about 4% for Ge on Si. These values of the lattice mismatch are critical in determining the growth mode of SAQDs because the growth process is largely driven by strain considerations resulting from that lattice mismatch.

Within the III-V compounds, considerable work has been done on the InAs/GaAs system.[1,2] Scanning tunneling microscope (STM) and atomic force microscope (AFM) images indicate that arrays of these dots can be grown with diameters typically of the order of 25 nm, with a size fluctuation of between five and seven percent of that diameter. Typical dot densities are of the order of 10^9 to $10^{11}/cm^2$. By observing optical emission from individual dots, a number of investigators have independently shown that these dots are indeed zero-dimensional quantum confined structures for electrons and holes. A variety of

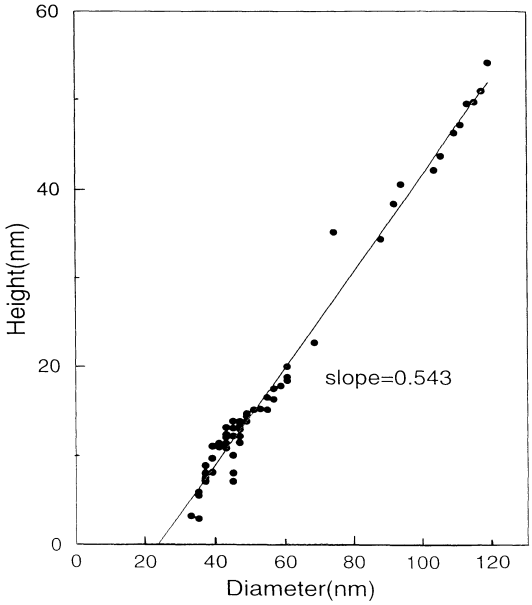

Figure 1. Dependence of height on diameter for CdSe dots on ZnSe. Note the linear dependence that extrapolates to 23nm diameter at zero height, indicating the error due to AFM tip diameter. The slope of 0.543 gives the aspect ratio.[6,7]

techniques has been used to reduce the number of quantum dots observed in these studies from values exceeding 10^6 to just a few hundred dots, for which strong emission from single dots can be observed, showing the δ-function-like characteristic expected from a zero-dimensional structure. Examples of these experiments include luminescence excitation with an electron beam (cathodoluminescence) using small apertures over the surface of the sample, or etching away all dots except a limited number contained on mesas.

In the case of the II-VI compounds, several laboratories have been investigating the growth of CdSe on ZnSe,[1-9] and self-assembled islands are again observed. In this case the growth temperature is considerably lower than for the III-Vs, on the order of 370 °C, and typical dot sizes or islands appear to be somewhat larger, as will be discussed below. Dot densities of a few times $10^9/cm^2$ have been observed. Uncapped CdSe dots are not stable on the ZnSe surface; detailed AFM studies have shown that they undergo Ostwald ripening[12] at room temperature. Study of this ripening process has been carried out in detail.[6,7] It has been demonstrated that all of the islands immediately after growth are of apparent size of approximately 55 nm. However, some of the dots subsequently grow in size at the expense of others. Figure 1 shows the height of a large number of these dots, measured by AFM, as a function of their diameter, regardless of the extent of ripening that has already taken place. All of the data points fall on a straight line

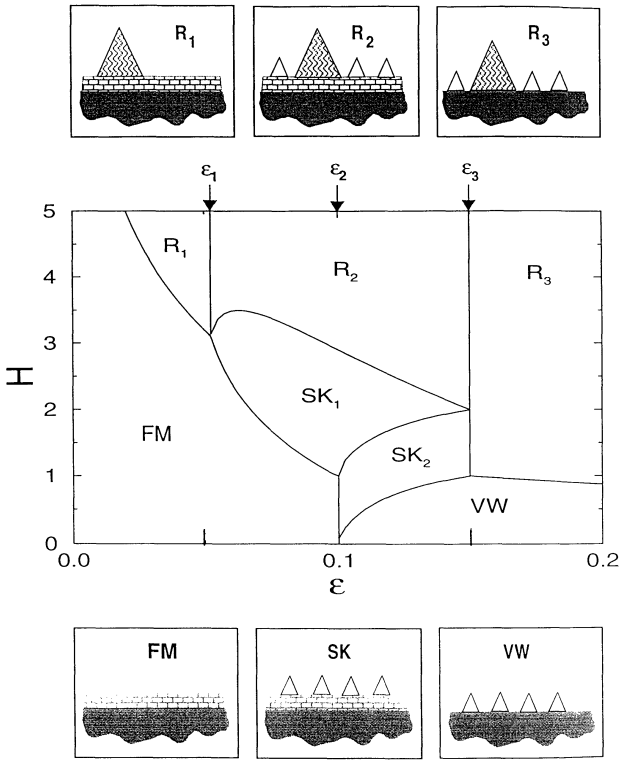

Figure 2 Equilibrium phase diagram for SAQD formation in function of the coverage (H) and lattice mismatch (ε). The small panels on the top and the bottom illustrate the morphology of the surface in the six growth modes. The small empty islands indicate the presence of stable islands, while the large shaded ones refer to ripened islands.[13]

that extrapolates at zero height to a diameter of approximately 23 nm. The fact that this line does not go through zero is a result of the finite size of the tip of the AFM machine. The dot diameter immediately after growth is therefore approximately 55-23 32 nm. Interestingly, the dots are highly stable at 0 °C.

In order to understand the growth mechanism, an equilibrium study of dislocation-free island formation has been carried out by Daruka and Barabási.[13,14] The results are summarized in the phase diagram shown in Fig. 2, which presents the possible growth modes in functional relationship to the number of monolayers deposited (H) and the lattice mismatch (ε). The phase diagram distinguishes a number of different growth mechanisms, including two-dimensional (2D) growth (or layer-by-layer growth), various kinds of Ostwald ripening indicated by R_I (I = 1 to 3), Stranski-Krastanow (SK), and Volmer-Weber (VW) growth. The 2D, SK,

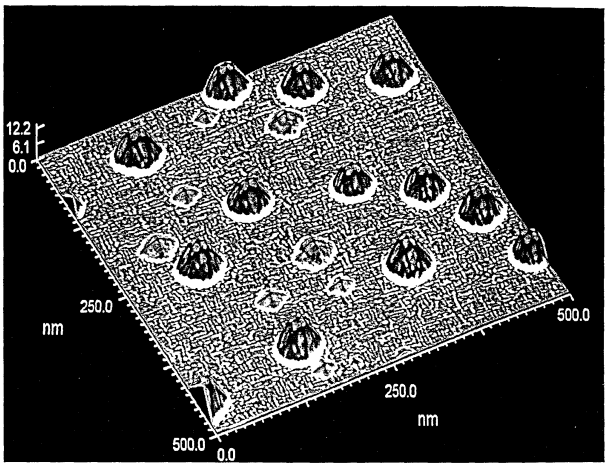

Figure 3. In situ scanning tunneling microscope image of 8 equivalent monolayers of Ge deposited onto Si(001) at 600 °C by physical vapor deposition, which shows the coexistence of both Ge pyramids and domes on the surface. In this image, the different facets are keyed to different shades of gray and the edges are enhanced by including a component of the local Laplacian in the shading of the image.

or VW growth modes generate stable islands, whereas three different kinds of ripening which may or may not include a two-dimensional layer (frequently called the wetting layer) are possible. This diagram demonstrates that in order to achieve stable and controllable SK or VW growth, for which uniform small islands may result, it is necessary to employ semiconducting crystal systems that include a large amount of strain (i.e., work far out along the horizontal axis in this diagram), and the deposited material must not exceed a certain critical coverage. For the systems already described (InAs/GaAs and CdSe/ZnSe), it appears that growth has taken place in the region $0.05 < \varepsilon < 0.1$, resulting either in a 2D-to-ripening transition for CdSe on ZnSe,[6,7] or possibly SK growth for InAs on GaAs.

Because of its compatibility with silicon microelectronic VLSI, a more interesting system is Ge on Si. Typically,[15] an array of dots is observed with average heights of 15 nm, a standard deviation less than 1 nm and a dot density of 6×10^9 cm^{-2}. However two different kinds of islands are usually seen, as shown in Fig. 3. If 8 monolayers of Ge are deposited on Si by physical vapor deposition (e.g., MBE), both small pyramidal islands, with the base of the pyramid of order 20 to 25 nm, and larger dome-shaped islands that exceed 50 nm are observed.[16] If growth is stopped after only four monolayers of Ge, most of the islands are the small pyramid type. The distribution of island sizes is shown in Fig. 4, where the distributions of smaller pyramids and larger domes are shown as a function of island volume. Both of these island types (pyramids and domes) are larger than

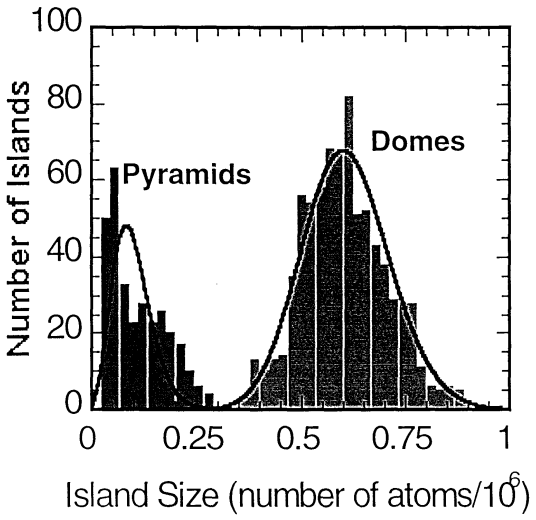

Figure 4. The histograms are the experimentally measured volume distributions of the pyramids and domes measured from high-resolution STM topographs of the same sample as Figure 5. The solid lines are the fits to the experimental data using the theory of Shchukin *et al*.[17]

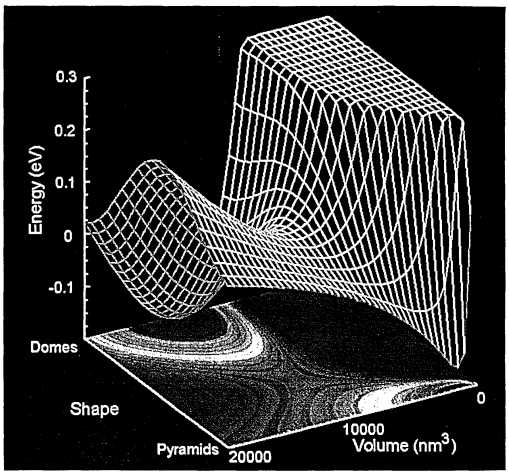

Figure 5. Internal free energy per atom *vs.* size and shape for Ge nanocrystals on Si(001). The volume dependence for the pyramids and domes was determined from the fit of Fig. 4. The shape axis is the reaction coordinate Γ taking a pyramid ($\Gamma = 0$) to a dome ($\Gamma = \pi$). The functional form for the plot along the shape axis is $E_a \sin^2[\Gamma]$ added to a linear interpolation between the energies of the limiting shapes. The saddle point represents the transition state of the shape change.

desired for quantum-confined systems to be of use for electronic applications, but considerable information about growth mechanisms has resulted from this systematic study.

An experimental STM study of the mechanism of Ge growth on Si showed that the size distributions of the pyramids and domes was consistent with a Boltzmann distribution applied to the free energy prediction of Shchukin *et al*.[17] A fit to experimental data, including the activation barrier for the shape transition, yields the free energy plot shown in Fig. 5; this plot reveals energy minima for both pyramids and domes as a function of the volume of the islands, and the activation barrier as a function of the shape parameter.

3. Nucleation control

In order for SAQDs to be useful from a practical point of view, it is essential to control the nucleation of these islands, because an ordered array of small dots that are equal in size is required for most applications. The size of the dots can be controlled either by strain resulting from the lattice mismatch of the system, as described above, or by limiting the source of atoms. For example, one can limit the surface area from which atoms are available for the growth of a single dot by fixing nucleation centers with spacing of the order of the surface diffusion length of these atoms. One can also order the array of resulting dots by some sort of coded or directed assembly procedure, by which nucleation sites are produced through some sort of surface patterning process. An example is shown in Fig. 6.

The upper part of this figure shows six simulated dot arrays, three of which result when growth is initiated on an unpatterned substrate, and three for which the substrate has been pre-patterned.[18] Three different values of growth flux have been used, F = 0.03, 0.08, 0.3 ml/s, for which the diffusion length of surface atoms (l_d) is taken to be greater than, approximately equal to, or less than the pattern spacing, respectively. (Note that l_d decreases with increasing F, and increases with increasing growth temperature).[19] The fluctuation in island size resulting in the case of substrate patterning is shown by the curve at the bottom of Fig. 6, which plots the normalized width of the dot size distribution as a function of flux. The square points indicate the case of no patterning. These simulations show that if the substrate is patterned with ordered nucleation sites separated by a distance l_i, then the fluctuation in island sizes varies significantly, depending on the size of the dot spacing relative to the diffusion length, with a sharp minimum at $l_d \quad l_i$. Thus, if the substrate can be patterned with spacing comparable to the diffusion length, regularly spaced islands with a small and uniform size can be obtained. Since the diffusion length can be controlled with the temperature and flux, one can find an appropriate combination of T and F to obtain optimal growth conditions for any desired island size.

How can one pattern the substrate before growth? Two techniques have been suggested, (1) growth of narrow mesas on the substrate, so that SAQDs can form only on the top of a mesa that extends above a passivating oxide,[20] and (2) using

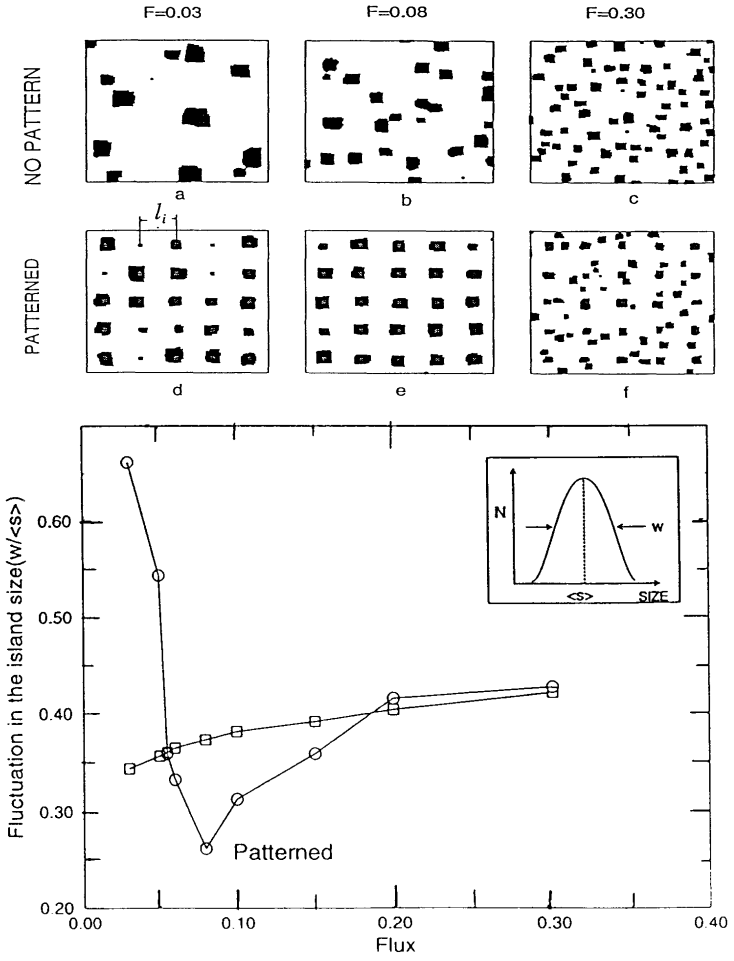

Figure 6. Top: Island morphologies obtained on an impurity-free substrate (a-c) as well as on a surface patterned with impurities (d-f) for coverage $\theta = 0.1$. The parameters in the Monte Carlo simulations are system size L = 400, $T = 400$ K, and $l_i = 40$. Bottom: Relative width of the island size distribution for surfaces without (A) and with impurities (B). W/<s> increases monotonously for the surface without impurities (A). In the presence of impurities, however, there exist a global minimum around F_{opt} 0.08.[18]

scanning probe techniques, such as STM or AFM, to produce nucleation sites. In the first case, nucleation sites tend to form equally-spaced along the mesa, because the formation of the mesa itself provides equal areas to serve as the source of atoms, as shown in Fig. 7. Two rows of regularly-spaced quantum dots are observed on each edge of the mesa. If the width of the mesa is increased, for

example to 670 nm or 1.0 micron, then additional rows of dots are formed, and the spacing of the dots is randomized, particularly for those that grow in the center of the mesa.[20]

An alternate technique for fixing nucleation sites employs scanning probe techniques, such as STM or AFM patterning. With the use of these scanning probes, one could (a) add foreign atoms, (b) remove host atoms, or (c) produce point defects or clusters, each of these serving as potential nucleation centers. The problem with this technique is that of *speed*; for a large array of dots, e.g., as might be needed for a modern VLSI architecture, it could take weeks, months, or even years to produce such a pattern by scanning probe techniques. However the speed by which scanning probes can be moved has been steadily increasing, with writing speeds up to 10 μm/s reported recently.[21] Also, there is ongoing research aimed at producing large numbers of parallel tips that can be controlled simultaneously.[22,23] The current state of the art involves 144 tips moving together. Any of these tips could be activated electrically, so that it should be possible to produce a pattern that is coded in a way to produce the desired circuit architecture. In general, it is possible that large-scale patterning by lithography combined with short-length-scale patterning by STM or AFM will provide the speed and reliability needed for applications such as quantum computers, lasers or detectors.

4. Applications

An important application for ordered arrays of SAQDs is the so-called quantum cellular automata (QCA) scheme developed by Lent and co-workers.[24] This

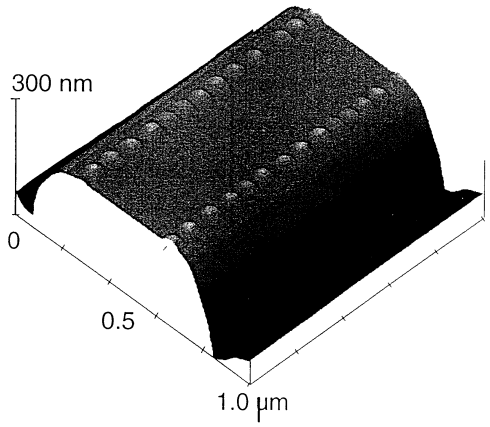

Figure 7. An atomic force microscope image of a 450 nm wide Si mesa oriented along a [100] axis of a (001) surface. The mesa was formed by growing Si on a surface that was patterned with a silicon dioxide film to restrict the regions where Si could grow. After formation of the mesa, Ge was deposited by chemical vapor deposition using germane. The Ge islands formed preferentially along the edges of the mesa.

application features arrays of quantum cells, each of which consists of either 4 or 5 quantum dots, with four dots occupying the four corners of a square. The cell is populated with two electrons that can tunnel between dots in a given cell, but cannot escape from the cell. The two possible ground states of this system would then be the two possible configurations of electrons opposite each other at the corners of the cell, as determined strictly by classical Coulomb repulsion. If one then fixes the configuration of one cell, the configuration of the neighboring cell is also fixed by Coulomb repulsion. It can be shown that the response function of this system, i.e. the response of one cell to its neighbor, is highly non-linear, which represents a kind of gain for the system. This nonlinearity permits the robust encoding of binary information in the state of the cell. Using this system, it has also been shown that all of the necessary logic operations for computing can be performed, and that this can be done in a highly efficient arrangement in terms of chip area.[25,26] For example, a full adder can be designed with approximately 200 of these cells (800 quantum dots) in a space less than 1.5 μm^2, whereas a full adder using conventional silicon CMOS technology would utilize 30 transistors at an average packing density of about 1.1 μm^2/transistor (using the SIA National Semiconductor road map for the year 2010). Furthermore, the highly complex multilevel metallization procedures now required for the wiring of conventional integrated circuits would be obviated because the QCA concept is truly a cellular automata system, such that contacts need only be made to an input plane and output plane—information propagates through the architecture in a fully automatic fashion.

Using conventional semiconductor quantum dots of the sort discussed earlier in this paper, for which typical nearest neighbor distances of these dots is of order 20 nm, the highly nonlinear switching function described above requires low-temperature operation (4 K). However, a molecular electronics implementation of this scheme is possible, for which the nearest neighbor distances are approximately 2 nm. In this case, the operational temperature of the system can increase by two orders of magnitude; i.e., operating temperatures well above room temperature are possible. A possible molecular implementation involves use of metal cluster carboxylates, as proposed by Cen *et al.*,[27] for which identical clusters involving the transition metals form square cells of the sort required. Research along these lines is currently proceeding at several laboratories.

5. Conclusions

In this paper we have described how the understanding of growth mechanisms of self assembled quantum dots has increased in recent years, and we described the current status for three semiconducting systems: (1) InAs/GaAs (III-V) technology, for which stable and uniform dots can be obtained, (2) CdSe/ZnSe (II-VI) dots, which show complicated ripening or coarsening phenomena, even at room temperature, and (3) Ge/Si (group IV) structures, whose growth shows a high degree of control, but the resulting dots are too large for quantum-

confinement purposes. We have described new methods for controlling uniformity that are being explored as well as methods to control (or code) the nucleation events. Finally, an application involving quantum cellular automata that could utilize semiconductors (if operated at low temperatures) or molecular-level structures (which operate at room temperature) was briefly described.

6. Acknowledgments

The authors wish to thank C. Lent for discussions on QCA, C.-S. Lee for providing Fig. 1, and T. I. Kamins for Fig. 7. The authors wish to thank the following agencies for support: J. L. M. was supported by DARPA/ONR (N00014-95-1-1166); A.-L. B. was supported by the ONR Young Investigator Program (N00014-98-1-0575); and J. K. F. was supported by the NSF (DMR 97-05064).

References

1. For up-to-date reviews see, e.g., W. Seifert, N. Carlsson, M. Miller, *et al.*, "In-situ growth of quantum dot structures by the Stranski-Krastanow growth mode," *J. Crystal Growth Character. Mater.* **33**, 423 (1996) and R. Nötzel, "Self-organized growth of quantum-dot structures," *Semicond. Sci. Technol.* **11**, 1365 (1996).
2. P. M. Petroff and G. Medeiros-Ribeiro, "Three dimensional carrier confinement in strain-induced self-assembled quantum dots," *MRS Bull.* **21** (4), 50 (1996).
3. S. H. Xin, P. D. Wang, Aie Yin, *et al.*, "Formation of self-assembling CdSe quantum dots on ZnSe by molecular beam epitaxy," *Appl. Phys. Lett.* **69**, 3884 (1996).
4. F. Flack, V. Nikitin, P. A. Crowell, *et al.*, "Near-field optical spectroscopy of localized excitons in strained CdSe quantum dots," *Phys. Rev.* B 54, R17312 (1996); see also F. S. Flack, A. Hunt, H. Hennessey, *et al.*, "Growth dynamics and exciton localization in strained CdSe quantum structures," *Mat. Res. Symp. Proc.* Vol. 417, Pittsburgh: Materials Research Society, 1996, p. 169.
5. J. Merz, S. Lee, and J. K. Furdyna, "Self-organized growth, ripening, and optical properties of wide-bandgap II-VI quantum dots," *J. Crystal Growth* **184/185**, 228 (1998)
6. J. K. Furdyna, S. Lee, I. Daruka, *et al.*, "Self-assembled growth of II-VI quantum dots," *Nonlinear Opt.* **18**, 85 (1997).
7. J. K. Furdyna, S. Lee, A.-L. Barabási, and J. L. Merz, "Self-organized low-dimensional II-VI nanostructures," to appear in: M. Tamargo, ed., *II-VI Semiconductor Materials and Their Application*, New York: Gordon and Breach, 1999.
8. K. Leonardi, H. Heinke, K. Ohdawa, *et al.*, "CdSe/ZnSe quantum structures grown by migration enhanced epitaxy: structural and optical investigations," *Appl. Phys. Lett.* **71**, 1510 (1997).

9. D. Hommel, K. Leonardi, H. Heinke, *et al*., "CdSe/ZnSe quantum dot structures: structural and optical investigations," *Phys. Stat. Sol. (b)* **202**, 835 (1997).
10. E. Kurtz, H. D. Jung, T. Hanada, *et al*., "The growth and photoluminescence properties of self-organized CdSe quantum dots on a (111)A ZnSe Surface," *Nonlinear Opt.* **18**, 13 (1997).
11. E. Kurtz, H. D. Jung, T. Hanada, *et al*., "Self-organized CdSe/ZnSe quantum dots on a ZnSe (111)A surface," *J. Crystal Growth* **184/185**, 248 (1998).
12. W. Ostwald, *Z. Phys. Chem. (Leipzig)* **34**, 495 (1990); for a review, see M. Zinke-Allmang, L. C. Feldman, and M. H. Grabow, "Clustering on surfaces," *Surf. Sci. Rep.* **16**, 377 (1992).
13. I. Daruka and A.-L. Barabási, "Dislocation-free island formation in heteroepitaxial growth: a study at equilibrium," *Phys. Rev. Lett.* **79**, 3708 (1997).
14. I. Daruka and A.-L. Barabási, "Equilibrium phase diagrams for dislocation free self-assembled quantum dots," *Appl. Phys. Lett.* **72**, 2102 (1998).
15. T. I. Kamins, E. C. Carr, R. S. Williams, and S. J. Rosner, "Deposition of three-dimensional Ge island on Si(001) by chemical vapor deposition at atmospheric and reduced pressures," *J. Appl. Phys.* **81**, 211 (1997).
16. G. Medeiros-Ribeiro, A. M. Bratkovski, T. I. Kamins, D. A. A. Ohlberg, and R. S. Williams, "Shape transition of germanium nanocrystals on a Si(001) surface from pyramids to domes," *Science* **279**, 353 (1998).
17. V. A. Shchukin, N. N. Ledentsov, P. S. Kop'ev, and D. Bimberg, "Spontaneous ordering of arrays of coherent strained islands," *Phys. Rev. Lett.* **75**, 2968 (1995).
18. C.-S. Lee and A.-L. Barabási, "Spatial ordering of islands grown on patterned surfaces," submitted to *Appl. Phys. Lett.* (1998).
19. A.-L. Barabási and H. E. Stanley, *Fractal Concepts in Surface Growth*, Cambridge, U.K.: Cambridge University Press, 1995.
20. T. I. Kamins and R. S. Williams, "Lithographic positioning of self-assembled Ge islands on Si(001)," *Appl. Phys. Lett.* **71**, 1201 (1997).
21. S. W. Park, H. T. Soh, C. F. Quate, and S.-I. Park, "Nanometer scale lithography at high scanning speeds with the atomic force microscope using spin on glass," *Appl. Phys. Lett.* **67**, 2415 (1995).
22. R. F. Service, "Meeting briefs: atomic landscapes beckon researchers," *Science* **274**, 723 (1996).
23. S. C. Minne, S. R. Manalis, and C. F. Quate, "Parallel atomic force microscopy using cantilevers with integrated piezoresistive sensors and integrated piezoelectric actuators," *Appl. Phys. Lett.* **67**, 3918 (1995).
24. Craig S. Lent, P. Douglas Tougaw, Wolfgang Porod, and Gary H. Bernstein, "Quantum cellular automata," *Nanotechnology* **4**, 49 (1993).
25. P. Douglas Tougaw and Craig S. Lent, "Logical devices implemented using quantum cellular automata," *J. Appl. Phys.* **75**, 1818 (1994).
26. Craig S. Lent and P. Douglas Tougaw, "A device architecture for computing with quantum dots," *Proc. IEEE* **85**, 541 (1997).
27. W. Cen, K. J. Haller, and T. P. Fehlner, "On the role of PES data in the identification of metal-metal charge transfer bands in clusters of clusters," *J. Electron Spectrosc.* **66**, 29 (1993).